Electronic Notes in Theoretical Computer Science 46 (2001)
URL: http://www.elsevier.nl/locate/entcs/volume46.html 18 pages

# "Honeycomb" vs Square and Cubic Models

Valentin E. Brimkov [1,2]

*Department of Mathematics*
*Eastern Mediterranean University*
*Famagusta, TRNC, Via Mersin 10, Turkey*

Reneta P. Barneva [3]

*Department of Mathematics and Computer Science*
*SUNY Fredonia*
*Fredonia, NY 14063, USA*

**Abstract**

In this paper we summarize some observations about the advantages of using hexagonal grids in raster graphics. We initiate a study of *honeycomb graphics*, whose 2D version is based on a hexagonal grid, while in its 3D counterpart the voxels are hexagonal prisms. We design an *analytical honeycomb geometry* of linear objects, which parallels similar developments already known in classical raster graphics [6]. We also demonstrate certain advantages of honeycomb graphics, in particular that it provides a better tunnel-free approximation to continuous objects.

## 1 Introduction

A tiling $\mathcal{P}$ of $\mathbb{R}^n$ by convex polytopes is called *normal* [7] if the intersection of any two tiles from $\mathcal{P}$ is either empty or appears to be their common $(n-d)$-dimensional facet, for some $d$, $1 \leq d \leq n$. Consider a normal tiling $\mathcal{P}$ of $\mathbb{R}^n$, $n = 2$ or 3, by copies of the same tile $P$, so that the following conditions are met.

(i) $P$ is a convex set;

(ii) For any $P_1, P_2 \in \mathcal{P}$ there is a translation $\tau$ such that $\tau(P_1) = P_2$;

(iii) Let $p$ be a point of a tile $P \in \mathcal{P}$. Then the set of the duplicas of $p$ in all tiles from $\mathcal{P}$ form a lattice in $\mathbb{R}^n$.

[1] The authors thank Jean-Pierre Reveillès for reading an early version of this paper.
[2] Email: valentin.brimkov@emu.edu.tr
[3] Email: barneva@cs.fredonia.edu

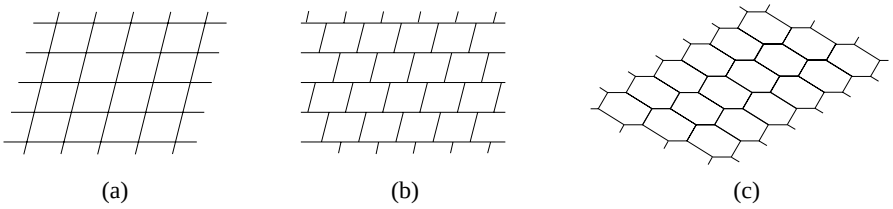


Fig. 1. a) Tiling by a parallelogram. b) Brick-built tiling. c) Tiling by a quasi-regular hexagon.

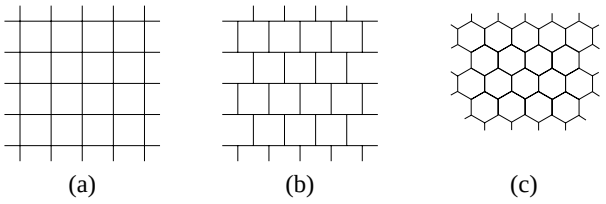


Fig. 2. a) Square grid. b) Regular brick-built grid. c) Regular hexagonal grid.

We will call such a tiling *uniform tiling*.

First we consider uniform tilings of $\mathbb{R}^2$. It is well-known (and also easy to see) that a uniform tiling is possible only in the following two cases.

- *Case 1:* The tile $P$ is a parallelogram (Figure 1a,b);
- *Case 2:* $P$ is a hexagon, whose opposite sides are equal and parallel. Such a hexagon will be called *quasi-regular* (Figure 1c).

The vertices and sides of the tiles form a *grid*. The *center* of a tile is the intersection point of its diagonals. Sometimes we will identify a tile with its center.

A grid can be regarded as an infinite plane graph $G = (V, E)$ whose vertex set $V$ and edge set $E$ consist of the polygons' vertices and sides, respectively. Note that the graph of the hexagonal grid of Figure 1c is isomorphic to the one of the parallelogram tiling of Figure 1b. Thus, these two grids have the same topology, despite the different shape of their tiles. A tiling/grid as the one in Figure 1b will be called a *brick-built tiling/grid*.

If we require the tiles to be regular polygons, then we obtain the *square grid* depicted in Figure 2a, the *regular brick-built grid* of Figure 2b, and the *regular hexagonal grid* of Figure 2c.

Similar considerations take place if we consider uniform tilings of $\mathbb{R}^3$. It is not hard to see that in this case the tile $P$ must be either a parallelepiped (Figure 3a) or a hexagonal prism whose bases are quasi-regular hexagons (Figure 3b). The notions of grid and tile center are defined analogously to the 2D case.

Square and cubic models in $\mathbb{R}^2$ and $\mathbb{R}^3$ are widely used in image processing and computer graphics. The raster computer graphics is modeled upon a square grid, where the square tiles are usually called *pixels*. Square grids are physically implemented in the computer screen. In dimension three, the

Fig. 3. The two possible tiles of a uniform tiling of $\mathbb{R}^3$.

graphical models are based on cubic grids, in which the cubes are called *voxels*.

Comparatively less attention has been paid to hexagonal grids and graphical models based on them. In the present note we attempt to show that this is, to a certain extent, undeserved. What is more, we will show that graphical models using hexagonal grid tiles (called *2-hexels*) have some advantages over the traditional ones. Similar conclusions hold for the 3D space, where instead of cubes, one can use voxels, which are hexagonal prisms (called *3-hexels*). Graphical models based upon hexels will be called *honeycomb models*. The basic aim of this work is to provide motivation and theoretical grounds for developing honeycomb graphics. Note that the proposed models are realistic and admit an easy hardware implementation. In fact, hexagonal rasters are well-known in image processing (see, e.g., [8]). Here we will show that:

- The proposed honeycomb models employ *simple mathematics*.
- In some regards, they are *"more economic"* than those based on square/cubic grids.
- Some basic Euclidean primitives (like straight lines, segments, polygons, circles, planes, etc.) admit a *simple analytical description*.
- Honeycomb models *ensure tunnel-freedom* of discrete objects in a more direct way than the other models.
- They ensure a *better tunnel-free approximation* to continuous objects.
- There is a possibility for a *straightforward transfer of notions and results* from the classical discrete geometry to one based on honeycomb models.

The paper is structured as follows. In the next Section 2 we recall some definitions and introduce notions to be used in the sequel. In Section 3 we provide theoretical foundations for developing 2D discrete analytical geometry of linear objects and circles. We also reveal some advantages of our approach over the classical one. In Section 4 we extend our considerations to the 3D space. In Section 5 we concern algorithmic and complexity issues. In the last Section 6 we conclude with some remarks.

The presented theory parallels in part some concepts and results already known in conventional raster graphics. Therefore, we omit the unnecessary details and focus on the essential differences, resemblances and advantages with respect to the classical theory. An important purpose of ours is to make the considered notions and facts intuitively clear. With this in mind, we often avoid technical details and calculations, using instead illustrative figures and examples. Observations and statements whose verification is either straightforward or quite technical or both, are left for exercise.

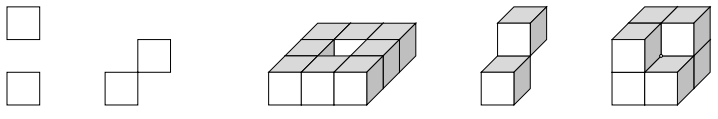


Fig. 4. Illustration to Definition 1 in the case of square/cubic tiles: a) Tunnels in a 2D discrete object. (i) 1-tunnel, (ii) 0-tunnel. b) Tunnels in a 3D object: (i) 2-tunnel, (ii) 1-tunnel, (iii) 0-tunnel.

## 2 Basic Definitions and Facts

Let $\mathcal{T}$ be a normal tiling of $\mathbb{R}^n$, where $n = 2$ or 3. We assume that the tiles of $\mathcal{T}$ are convex polytopes. For a set of tiles $A$ we denote $U(A) = \cup_{P \in A} P$. A set of tiles will be regarded as a *discrete object*.

A $j$-dimensional facet of a tile $P \in \mathcal{T}$ will be called *$j$-facet*, for some $j$, $0 \leq j \leq n-1$. Thus the 0-facets of $P$ are its vertices, the 1-facets are its edges, and the 2-facets of a 3D polytope are its 2D faces.

Two tiles are called *$j$-adjacent* if they share a $j$-facet. A *$k$-path* in a discrete object $A$ is a sequence of tiles from $A$ such that every two consecutive tiles are $k$-adjacent. Two tiles are *$k$-connected* if there is a $k$-path between them. A discrete object $A$ is *$k$-connected* if there is a $k$-path connecting any two tiles of $A$. A discrete object is said to be *connected* if it is at least 0-connected. Otherwise it is *disconnected*.[4]

Let $D$ be a subset of a discrete object $A$. If $A - D$ is not $k$-connected then the set $D$ is said to be *$k$-separating* in $A$. A *supercover* of an Euclidean object $M$ is the set $S(M)$ of all tiles which are intersected by $M$. Let $\Gamma$ be a curve in $\mathbb{R}^2$ or a surface in $\mathbb{R}^3$. In a very general sense, one can consider every subset of the supercover $S(\Gamma)$ as a *discretization* of $\Gamma$, or as a *discrete curve/surface* corresponding to $\Gamma$. An important concept in discrete geometry for computer imagery is that of *tunnel*. Intuitively, a *$k$-tunnel* is a location in a discrete object through which a discrete $k$-path can penetrate. Tunnels in a discrete object (in particular, discrete curve or surface), are usually defined on the basis of the notion of separability. More precisely, let a set of tiles $A$ be $k$-separating in a discrete object $B$ but not $j$-separating in $B$. Then $A$ is said to have $j$-tunnels for any $j < k$. In the case when the considered set $A$ (discrete curve in $\mathbb{R}^2$ or discrete surface in $\mathbb{R}^3$) is not supposed to be separating in another set, one can use the following somewhat more general definition.

**Definition 2.1** Let $A$ be a discrete object in $\mathbb{R}^n$, where $n = 2$ or 3.

[4] Classically, 0-adjacent/connected (resp. 1-adjacent/connected) pixels are called 8-adjacent/connected (resp. 4-adjacent/connected). In dimension 3, 0-adjacent/connected (resp. 1 or 2-adjacent/connected) voxels are called 26-adjacent/connected (resp. 18 or 6-adjacent/connected).

a) If $n = 2$, then:

(i) $A$ has a 1-tunnel if the set $U(A)$ is disconnected (Figure 4a(i));

(ii) $A$ has a 0-tunnel if in $A$ there exist two tiles which share exactly one vertex, and no other tile from $A$ shares the same vertex (Figure 4a(ii)).

b) If $n = 3$, then:

(i) $A$ has a 2-tunnel if $U(A)$ is not a simply connected set (Figure 4b(i)); (Such kind of tunnel is sometimes called a *hole*.)

(ii) $A$ has a 1-tunnel if in $A$ there exist two tiles which share exactly one edge, and no other tile from $A$ shares the same edge (Figure 4b(ii));

(iii) $A$ has a 0-tunnel if it contains a tile $P$ which has a vertex $q$, so that the set $U(A) - q$ is not simply connected (Figure 4b(iii)).

Discrete object without $k$-tunnels is called *$k$-tunnel-free*. An object that has no tunnels for any $k$, $0 \leq k \leq 2$, is called *tunnel-free*, for short. [5]

The notion of tunnel plays an important role in rendering voxelized scenes by casting discrete rays from the image to the scene [5]. As Kaufman remarks, thinner rays are much more attractive for ray traversal. Therefore, it is desirable to construct $k$-tunnel-free discrete objects where $k$ is as small as possible. The ideal situation is when the object is tunnel-free. The 2D case is comparatively simple since the connectivity of a discrete object fully characterizes the topology of the tunnels. More precisely, an object $A$ contains 1-tunnels if and only if it is disconnected; $A$ contains 0-tunnels but no 1-tunnels if and only if it is connected but not 1-connected; $A$ is tunnel-free if and only if it is 1-connected. In dimension 3, however, the situation is more complicated, as one can deduce from the definition above. Sometimes this complexity has certain negative impact on the design of discretization algorithms. In particular, it may be difficult to control the object connectivity. Moreover, it might even be a problem to secure that a discrete object is connected [2]. Ensuring tunnel-freedom can be a difficult task as well [2,3,4].

A source for such sort of troubles is the topology of the square grid. Still in dimension 2, there are three possibilities for connectivity of two pixels, and thus for the tunnel structure of a set of two pixels. In dimension 3, the corresponding number of cases is four (0, 1, 2-tunnel, and tunnel-freedom). This variety of possibilities may cause certain theoretical difficulties when constructing $k$-tunnel-free discretizations of more complex objects. In Sections 3 and 4 we will show how one can overcome this problem by using honeycomb models. Before this, we recall some basic concepts of the analytical discrete geometry.

[5] Classically, in dimension two, a 0-tunnel (resp. 1-tunnel) is called 8-tunnel (resp. 4-tunnel). In dimension three, a 0-tunnel (resp. 1- or 2-tunnel) is called 26-tunnel (resp. 18- or 6-tunnel).

*Analytical Discrete Geometry*

A novel approach in raster graphics is the one based on analytical discrete geometry [6]. The main objective here is to obtain simple analytical definitions of the basic Euclidean primitives, such as lines and line segments, triangles, circles, planes, spheres, etc., and, on this basis, to create tools for efficient modeling of more sophisticated objects composed by these primitives. Next, we recall some basic definitions.

*Discrete coordinate plane* consists of unit squares (pixels), centered on the integer points of the two-dimensional Cartesian coordinate system in the plane. *Discrete coordinate space* consists of unit cubes (voxels), centered on the integer points of the three-dimensional Cartesian coordinate system in the space. The pixels'/voxels' coordinates are the coordinates of their centers. The edges of a pixel/voxel are parallel to the coordinate axes.

*2D arithmetic line* is a set of pixels $L(a_1, a_2, \mu, \omega) = \{(x, y) \in \mathbb{Z}^2 | 0 \leq a_1x + a_2y + \mu < \omega\}$, where $a_1, a_2, \mu \in \mathbb{Z}$, $\omega \in \mathbb{N}$. $\omega$ is called *arithmetic thickness* or *width* of the line and $\mu$ is called *internal translation constant*. The vector $(a_1, a_2)$ is the *normal vector* to the line. An arithmetic line $L(a_1, a_2, \mu, \omega)$ is *0-connected* (classically, *8-connected* or *naive*) if $\omega = \max(|a_1|, |a_2|)$, and *1-connected* (classically, *4-connected* or *standard*), if $\omega = |a_1| + |a_2|$. The standard line is the thinnest tunnel-free arithmetic line. *Arithmetic plane* is a set of voxels $P(a_1, a_2, a_3, \mu, \omega) = \{(x, y, z) \in \mathbb{Z}^3 | 0 \leq a_1x + a_2y + a_3z + \mu < \omega\}$, where $a_1, a_2, a_3, \mu \in \mathbb{Z}$, $\omega \in \mathbb{N}$. $\omega$ is the *arithmetic thickness* of the plane and $\mu$ is its *internal translation constant*. The vector $(a_1, a_2, a_3)$ is the *normal vector* to the plane. An arithmetic plane $P(a_1, a_2, a_3, \mu, \omega)$ is *naive* if $\omega = \max(|a_1|, |a_2|, |a_3|)$, and *standard* if $\omega = |a_1| + |a_2| + |a_3|$. The standard plane is the thinnest tunnel-free arithmetic plane.

## 3 2D Honeycomb Analytical Geometry

### *3.1 Hexagonal Coordinate System*

Consider the tilings of Figure 2c and 2b. As mentioned, the corresponding grids are isomorphic. An important property of these tilings is that any two non-disjoint tiles are 1-adjacent. In contrast to the case of classical rectangular grids, here 0-adjacency is impossible. Thus, a connected discrete object is always 1-connected and tunnel-free. We will now develop a basis for analytical discrete geometry on hexagonal grids.

The centers of the 2-hexels form a lattice $L$ whose cells are unit rhombuses (see Figure 5a). The hexels form a *discrete hexagonal space*. On it, we define a *hexagonal coordinate system*. For this, we choose a hexel and define its center $O$ to be the center of the coordinate system. The center's coordinates are both zeros, i.e., $O = (0, 0)$. Next we fix two coordinate axes as shown in Figure 5a. The basis vectors $b_1$ and $b_2$ of the system are the vectors of the lattice basis, aligned with the coordinate axes. The so defined hexagonal coordinate system

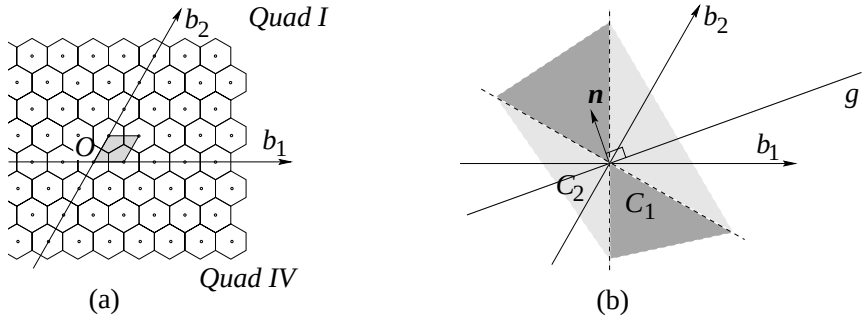


Fig. 5. a) Hexagonal coordinate system. b) The Quad I,II,III,IV and the cones $C_1$ and $C_2$. The normal vector $\mathbf{n} = (a_1, a_2)$ to the straight line $g$ belongs to $C_1$.

will be denoted by $Ob_1b_2$.

The coordinate axes $Ob_1$ and $Ob_2$ divide the plane into four quadrants, denoted *Quad I*, *Quad II*, *Quad III*, and *Quad IV*. The origin $O$ is common for *Quad II* and *Quad IV*. The positive part of $Ob_1$ and the negative part of $Ob_2$ belong to *Quad IV*, while the positive part of $Ob_2$ and the negative part of $Ob_1$ belong to *Quad II*. With respect to the coordinate system $Ob_1b_2$, one can build an analog of the Cartesian analytical geometry.

### *3.2 Lines, Segments, and Polygons*

Let $a_1x_1 + a_2x_2 + b = 0$ be the equation of a straight line $g$ in the hexagonal coordinate plane. We will suppose that the coefficients $a_1, a_2$, and $b$ are rational numbers. To simplify some considerations, we will assume that they are integers and that $gcd(a_1, a_2)$ divides $b$. This ensures that the line $g$ contains infinitely many equidistant lattice points. The vector $\mathbf{n} = (a_1, a_2)$ is the *normal vector* to $g$. The line $g$ is collinear with the vectors $v' = (a_2, -a_1)$ and $v'' = (-a_2, a_1)$. The normal vectors to straight lines $g$ for which the vectors $v'$ and $v''$ belong to *Quad I* and *Quad III*, form an open cone $C_1$ (Figure 5b). Analogously, the normal vectors to straight lines $g$ for which the vectors $v'$ and $v''$ belong to *Quad II* and *Quad IV*, form a closed cone $C_2$ (Figure 5b). Clearly, $C_1 \cap C_2 = \emptyset$ and $C_1 \cup C_2 = \mathbb{R}^2$.

We now define a *universal discrete line* corresponding to $g$, as follows.

$$g^D(a_1, a_2, b) = \{x \in L : 0 \leq a_1x_1 + a_2x_2 + b + \lfloor t/2 \rfloor < t\},$$

where

$$t = \begin{cases} |a_1| + |a_2|, \text{ if } \mathbf{n} = (a_1, a_2) \in C_1, \\ \max(|a_1|, |a_2|), \text{ if } \mathbf{n} = (a_1, a_2) \in C_2. \end{cases}$$

See Figure 6.

The parameter $t$ is called the *universal width* of the line $g^D$. It equals the number of parallel equidistant straight lines, which contain centers of hexels from $g^D$.

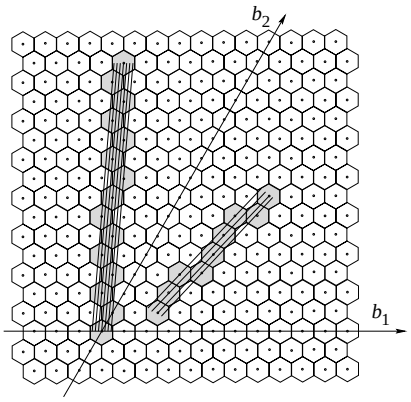


Fig. 6. Two discrete line segments. The one has end-points $(2, 1)$ and $(4, 7)$, while the other has end-points $(0, 0)$ and $(-6, 14)$. The normal vector to the former belongs to the cone $C_1$. This discrete line does not have the containment property. The normal vector to the latter belongs to the cone $C_2$. This discrete line has the containment property.

The so defined discrete line $g^D$ is *the thinnest possible* connected line of this type. For smaller values of $t$ the line becomes disconnected, while for larger values it contains extra hexels which, however, do not influence the line connectivity. We remark that, depending on the quadrant to which the normal vector belongs, the universal width equals the thickness $\omega$ of a standard or a naive line in a square grid (see Section 2). Note also that, if $t = |a_1| + |a_2|$, then the discrete line has *containment property* [5], i.e., it fully contains the corresponding continuous line. If $t = \max(|a_1|, |a_2|)$, then the containment property does not hold, in general.

Given two hexels $h_1$ and $h_2$, one can obtain a tunnel-free discrete segment with end-points $h_1$ and $h_2$. In the same way, one can construct tunnel-free discrete polygons.

### *3.3 Discrete Circles*

The circle is another basic Euclidean primitive admitting an easy analytical definition. In a square grid, a discrete circle has been analytically defined in [1]. More precisely, one can consider the following discrete circle with center at $O(0, 0)$ and radius $r \in \mathbb{N}$.

$$C(r) = \left\{ (x, y) \in \mathbb{Z}^2 : \left( r - \frac{1}{2} \right)^2 \leq x^2 + y^2 < \left( r + \frac{1}{2} \right)^2 \right\}. \qquad (1)$$

Note, however, that the above definition cannot be directly applied to a hexagonal grid since it may define a set of hexels which is too far from the intuitive idea of a circle and, in fact, can be a disconnected set of hexels (see Figure 7a). Therefore, a new definition is needed. To this end, we first observe that a point $(a, b)$ in the hexagonal coordinate system has coordinates

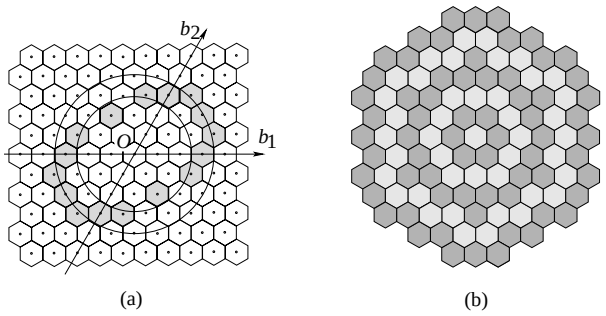


Fig. 7. a) The set of hexels satisfying condition (1) with $r = 3$. b) Concentric discrete circles defined by formula (2), for $r = 1, 2, 3, 4, 5$.

$(a + \frac{b}{2}, \frac{\sqrt{3}}{2}b)$ with respect to the square coordinate system with the same unity. Then the equation of a Euclidean circle in the hexagonal system becomes

$$\left(x + \frac{y}{2}\right)^2 + \left(\frac{\sqrt{3}}{2}y\right)^2 = r^2,$$

i.e.,

$$x^2 + xy + y^2 = r^2.$$

Thus we obtain the following analytical definition of a discrete circle with center $O(0, 0)$ and radius $r$.

$$C^D(r) = \left\{(x, y) \in L : \left(r - \frac{1}{2}\right)^2 \leq x^2 + xy + y^2 < \left(r + \frac{1}{2}\right)^2\right\}. \quad (2)$$

See Figure 7b.

It is not hard to realize that the so defined discrete circle is always connected and tunnel-free. Moreover, concentric discrete circles with radii $r = 1, 2, 3, \ldots$ fill the whole plane.

### *3.4 Optimality of the Honeycomb Model*

To have a ground for comparison between models built upon square or hexagonal grids, we will suppose that the square and the hexagonal tiles have the same area 1. We will call such tiles the *unit square* and the *unit 2-hexel*, respectively. One can calculate that the length of a side of the unit 2-hexel is equal to

$$a = \frac{\sqrt{2}}{\sqrt{3}\sqrt[4]{3}} = 0.62040\ldots.$$

#### *3.4.1 Quality of Approximation*

We will show next that in certain sense the hexagonal grid ensures a better approximation to a continuous line segment than the square and the brick-built grids. To this end, we first recall the definition of Hausdorff distance. Let

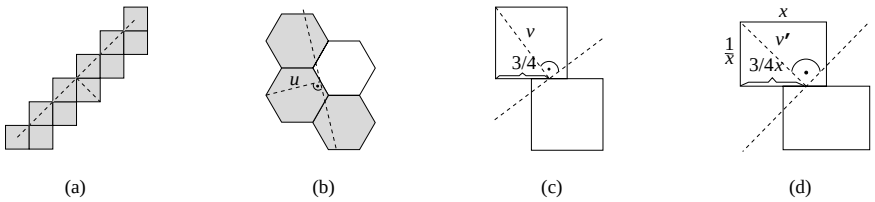


Fig. 8. Extreme cases for which a 2-hexel of a discrete line has maximal deviation from the continuous line. a) In a square grid. b) In a regular hexagonal grid. c) In a regular brick-built grid. d) In the optimal brick-built grid.

$E$ be a metric space with metric $d$, and $\mathcal{E}$ a family of closed non-empty subsets of $E$. For every $x \in E$ and every $A \in \mathcal{E}$ let $d(x, A) = \inf\{d(x, y) : y \in A\}$. Then, given two sets $A, B \in \mathcal{E}$,

$$H_d(A, B) = \max\{\sup\{d(a, B) : a \in A\}, \sup\{d(A, b) : b \in B\}\}$$

is called the *Hausdorff distance* between $A$ and $B$. We will suppose that $d$ is the Euclidean metric.

We will measure the *deviation* of a straight line discretization $g^D$ from the corresponding continuous line $g$ by the Hausdorff distance $H_d(g^D, g)$ between them.

We first compare the hexagonal and the square grids. As Figure 8a shows, a tunnel-free discrete line might contain pixel (or pixels) whose farthest point is in a distance $\sqrt{2} = 1.41421\ldots$ from the line. Consider now the hexagonal grid. For it, the maximal possible deviation is reached in the extreme case illustrated in Figure 8b. It is equal to

$$u = \frac{\sqrt{13}}{2}a = \frac{\sqrt{13}}{2}\frac{\sqrt{2}}{\sqrt[4]{27}} = 1.11844\ldots,$$

which is considerably less than in the case of square grid.

Consider now the brick-built grid whose tiles are unit squares. For it, the maximal possible deviation is reached in the case shown in Figure 8c, and is equal to $v = 1.25$. This is smaller than the corresponding value for square grid, but larger than the one for hexagonal grid.

Note that in a brick-built grid framework, unit square tiles do not provide the best possible approximation. In order to determine the dimensions of the optimal rectangle, with reference to Figure 8d, let us denote the length of its horizontal side by $x$. Then the other side length will be $\frac{1}{x}$. Now we have to determine $x$ which minimizes the function

$$f(x) = \frac{1}{x^2} + \frac{3}{4}x^2.$$

Using simple calculus, we find that the solution to the above optimization

problem is

$$x = \frac{2}{\sqrt{3}} = 1.15470\ldots.$$

Then the other side has length $\frac{1}{x} = 0.86602\ldots$ A grid with such a tile will be called the *optimal brick-built grid*. For it, the maximal deviation is equal to

$$v' = \left(\left(\frac{1}{x}\right)^2 + \left(\frac{3}{4}x\right)^2\right)^{1/2} = 1.22474\ldots.$$

It is easy to show that the maximal deviation of a discrete line in a regular hexagonal grid is minimal over all quasi-regular hexagonal grids. Similarly, the maximal deviation of a discrete line in the optimal brick-built grid is minimal over all possible brick-built grids.

Thus, we have obtained that the regular hexagonal grid provides the optimal ground for constructing a tunnel-free approximation to a continuous linear object.

Similar results and conclusions hold about the maximal possible deviation of a discrete circle from the corresponding Euclidean circle.

### *3.4.2 Grid Cost*

We conclude this section with one more observation, namely that the hexagonal grid is in a sense "more economic" than the square one. For a given grid $H$, the total length of all its edges will be called the *cost* of $H$ and denoted $c(H)$. One can calculate that a unit 2-hexel has perimeter $6a = 3.72241\ldots$, which is less than the perimeter of the unit square, that is 4. This fact may have an advantageous impact on the cost of the corresponding grid, as illustrated through the following example.

**Example 3.1** Consider the grid of a screen with a square shape, consisting of $n$ rows, each of them containing $n$ unit tiles. We consider the cases of square grid $H_1$ (Figure 9a) and hexagonal grid $H_2$ (Figure 9b). Both grids cover the same area $n^2$. One can easily find that in the former case the grid cost is

$$c(H_1) = 2n^2 + 2n,$$

while in the latter case it is

$$c(H_2) = (3n^2 + 4n - 1)a = (3a)n^2 + 4an - a.$$

Since the coefficient of $n^2$ in $c(H_2)$ is $3a = 1.86120... < 2$, we obtain that $c(H_2)$ is asymptotically smaller than $c(H_1)$.

It is easy to show that a unit 2-hexel has a minimal perimeter among all quasi-regular hexagons with area 1. One can also show that a tiling by unit 2-hexels has minimal cost among all possible tilings by a quasi-regular hexagon with area 1. Similarly, a unit square has a minimal perimeter among

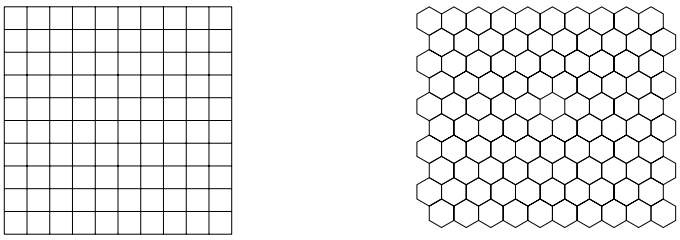


Fig. 9. Illustration to Example 3.1.

all parallelograms with area 1, and a tiling by a unit square has a minimal cost over all possible tilings by a parallelogram with area 1. Thus, one can conclude that the tiling with regular hexagons has minimal cost over all possible uniform tilings.

The above observation may be of interest regarding possible wire grid fabrication for the purpose of a novel computer screen design, based, e.g., on liquid-crystals, plasma panels, or electro-luminescent technologies.

## 4 3D Honeycomb Geometry

In this section we present two 3D honeycomb models and related discrete analytical geometry. In both of them the 3D space is tiled by a right hexagonal prism called 3-hexel (see Figure 11b). The base of the prism is a unit 2-hexel and its height has length 1. Thus the 3-hexel volume is equal to 1.

Our aim is to create a basis for tunnel-free discretizations of surfaces and lines, in particular of planes and straight lines. For this, we consider two special tilings of $\mathbb{R}^3$ by 3-hexels and define corresponding coordinate systems in them.

### *4.1 Model I*

Let $h_0$ be a 3-hexel in $\mathbb{R}^3$. Its center $O$ is assigned coordinates $(0, 0)$ and will be considered as the origin of the coordinate system. Consider a tiling of $\mathbb{R}^3$ as the one illustrated in Figure 10a,b. The figure exposes the orthogonal projections of the centers of a set of 3-hexels on the plane $\mathcal{P}$, passing through the origin $O$ and orthogonal to the hexel's height. We choose one of the coordinate axes to be the straight line $e_3$ passing through $O$ and orthogonal to $\mathcal{P}$. On every hexagonal projection the third coordinate of the corresponding 3-hexel's center is marked (i.e., the coordinate of the hexel's center with respect to $e_3$ axes). These centers belong to a plane which is chosen to be one of the discrete coordinate planes. In it, we fix the other two coordinate axes $e_1$ and $e_2$. The origin $O$ and the axes $e_1$, $e_2$, and $e_3$ determine the coordinate system $Oe_1e_2e_3$ (Figure 10b).

Now for each 3-hexel $h$ from the discrete coordinate plane $Oe_1e_2$, we tile

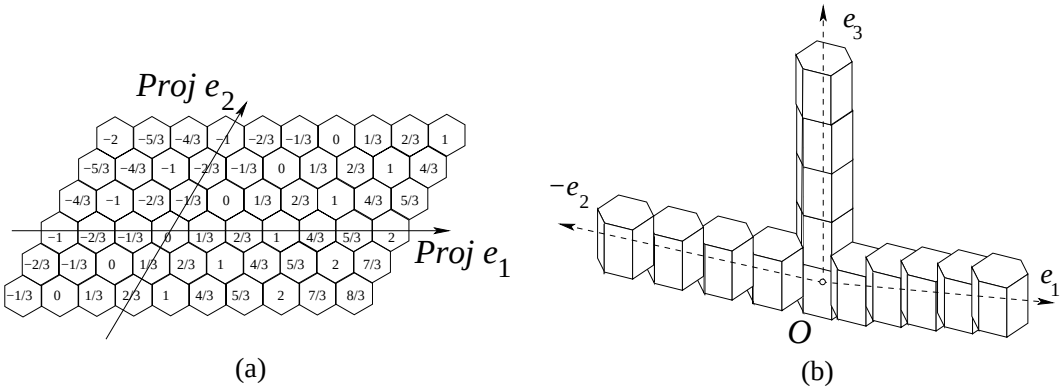


Fig. 10. Illustration to Model I. a) The orthogonal projections of the centers of 3-hexels on the plane $\mathcal{P}$. b) The axes of the coordinate system $Oe_1e_2e_3$. The rays $e_1$ and $-e_2$ make an angle of 120 degrees.

the space upward and downward by adjacent copies of $h$. Thus, we obtain a tiling of $\mathbb{R}^3$.

In the discrete coordinate plane $Oe_1e_2$ one can consider the four quadrants $QuadI$, $QuadII$, $QuadIII$, and $QuadIV$, determined by the coordinate axes.

By construction, the centers of the 3-hexels form a lattice $H$ in $\mathbb{R}^3$. Note that every two neighboring 3-hexels are 2-adjacent. No 0- or 1-tunnels are possible in a connected set of 3-hexels.

### *4.1.1 Analytical Discrete Plane*

Consider a Euclidean plane $P$ with equation

$$a_1x_1 + a_2x_2 + a_3x_3 = b, \quad a_1, a_2, a_3, b \in \mathbb{Z},$$

with respect to the defined coordinate system. Assume as before that $gcd(a_1, a_2, a_3)$ divides $b$, i.e., $P$ contains a 2-dimensional lattice $L$ which is a sublattice of $H$.

We now define a *universal discrete plane* corresponding to $P$, as the set

$$P^D(a_1, a_2, a_3, b) = \{x \in H : 0 \leq a_1x_1 + a_2x_2 + a_3x_3 + b + \lfloor t/2 \rfloor < t\}, \quad (3)$$

where

$$t = \begin{cases} |a_1| + |a_2| + |a_3|, \text{ if } \mathbf{n} = (a_1, a_2) \in C_1, \\ \max(|a_1|, |a_2|, |a_3|), \text{ if } \mathbf{n} = (a_1, a_2) \in C_2. \end{cases}$$

$C_1$ and $C_2$ are cones in the coordinate plane $Oe_1e_2$, defined analogously as before. The parameter $t$ is called the *universal width* of the plane $P^D$.

By the construction of the discrete space, the so defined discrete plane is always tunnel-free, and appears to be the thinnest possible tunnel-free discrete plane of this type. Similar to the 2D case, planes with thickness $t = |a_1| + |a_2| + |a_3|$ possess the containment property, while those with thickness $t = \max(|a_1|, |a_2|, |a_3|)$, in general, don't.

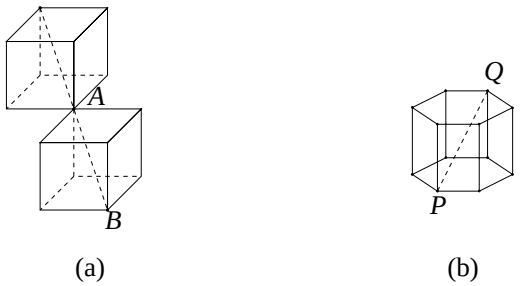


Fig. 11. a) The point $B$ is in a distance $\sqrt{3}$ from the Euclidean plane passing through the point $A$ and orthogonal to the straight line $AB$. b) The diagonal $PQ$ of a 3-hexel is shorter than the one of the unit cube, that is $\sqrt{3}$.

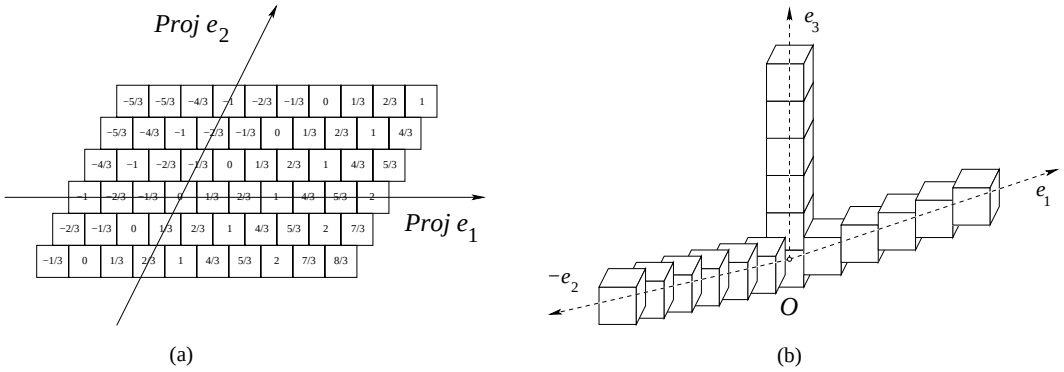


Fig. 12. Illustration to a brick-built version of model I.

*4.1.2 Optimality Issues*

First we remark that a 3-hexel has a total area of its surfels (faces) equal to

$$6 \times a + 2 \times 1 = 3.72241\ldots + 2 = 5.72241\ldots,$$

which is less than the one of the unit cube, that is 6. This leads to similar conclusions as in the 2D case regarding the grid cost, which can be defined as the total area of the surfels of the tiles involved.

Most importantly, the definition of a discrete plane within Model I ensures better approximation to the continuous plane compared to the classical cubic model. In fact, a tunnel-free standard plane may contain voxels that are in a distance $\sqrt{3}$ from the continuous plane (see Figure 11a), while within Model I this distance is clearly smaller. This can be immediately deduced from the fact that the longest diagonal of a 3-hexel is equal to

$$f = (1 + (2a)^2)^{1/2} = 1.59361\ldots,$$

which is less than $\sqrt{3} = 1.73205\ldots$ (see Figure 11b).

It is not hard to show that the right prism with a regular hexagonal base provides better approximation than the ones inclined and/or with quasi-regular hexagonal bases.

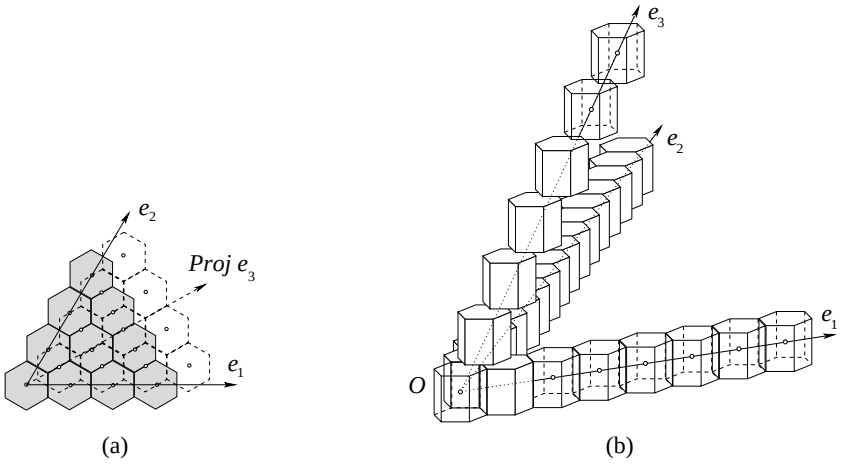


Fig. 13. Illustration to Model II. a) Projections of two consecutive slices of 3-hexels on the coordinate plane $Oe_1e_2$. b) The axes of the coordinate system $Oe_1e_2e_3$.

Similar considerations and conclusions hold for the case of brick-built models, when the hexagonal prisms are substituted by rectangular prisms (see Figure 12). One can show that with respect to the value of the maximal possible deviation from the continuous plane, the honeycomb model is superior to the brick-built one, while the latter is superior to the cubic model.

### *4.2 Model II*

Consider the regular hexagonal tiling of the plane. On every tile we build the corresponding 3-hexel. Thus we obtain a discrete plane $P_0$.

We fix one of the hexels and choose its center $O(0, 0)$ as origin of the coordinate system. Then we choose the axes $e_1$ and $e_2$ as in the 2D case. Thus we obtain one of the discrete coordinate planes, namely $Oe_1e_2$. We now build on the top of the discrete plane $P_0$ a next "slice," equivalent to $P_0$ and shifted as illustrated on Figure 13a. Proceeding analogously upward and downward, we obtain a tiling of $\mathbb{R}^3$. We notice that the tiles' centers constitute a lattice in $\mathbb{R}^3$.

We now determine the third axis $e_3$ as shown in Figure 13b. Similar to Model I, a connected set of 3-hexels is always 2-connected and does not contain any 0- and 1-tunnels. In the obtained discrete space, we can define with respect to the coordinate system $Oe_1e_2e_3$ a discrete plane in the same way as in the framework of Model I. One can see that it is always tunnel-free and is the thinnest possible tunnel-free discrete plane of this type. One can also show that a discrete plane defined by (3) provides a better approximation to the corresponding continuous plane (in terms of maximal deviation from the continuous plane) than the corresponding standard plane within the cubic model.

The comparison with the brick-built model (Figure 14) leads to similar conclusions as in the case of Model I. Discrete spheres can be defined and

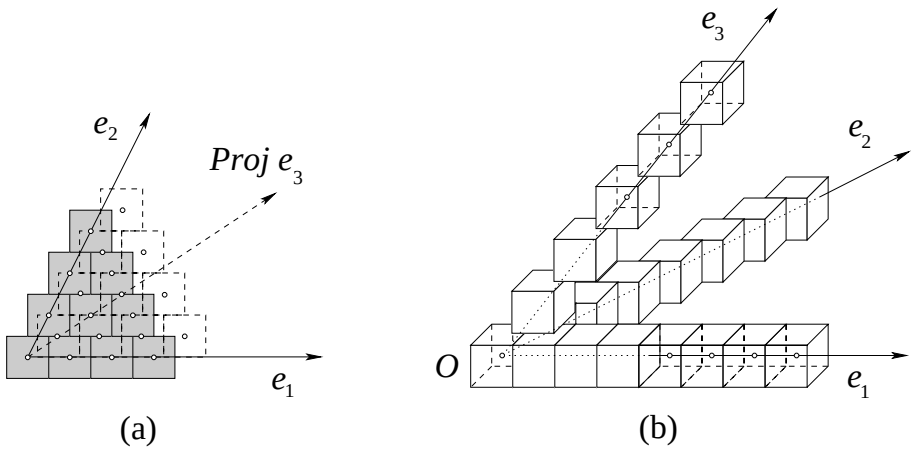


Fig. 14. Illustration to a brick-built version of Model II.

studied similarly to discrete circles.

We conclude the discussion on 3D honeycomb models with one more remark. In Model I, every 3-hexel $h$ of the 3D discrete space has fourteen 2-neighbors: one for the upper hexagonal face, one for the lower hexagonal face, and two for each one of the six side rectangular faces. In Model II, the structure of a 3-hexel neighborhood is completely different: there are four neighbors for every one of the two hexagonal faces and one for each of the six rectangular faces. Nevertheless, the overall number of neighboring 3-hexels is the same as in Model I, i.e., fourteen. It is not hard to show that the two neighborhood structures relative to Model I and Model II, respectively, are the only ones possible, under the condition that the tiling is uniform and any two adjacent tiles are 2-adjacent.

## 5 Algorithmic and Complexity Issues

The considered analytical discrete primitives (discrete straight lines and line segments, discrete circles and planes) admit an efficient algorithmic generation. They can be obtained in time that is linear in the number of the generated hexels. This can be done in several different ways. We will show that the well-known linear time algorithms that work in the framework of the square/cubic models, can be transferred straightforwardly to the case of the considered honeycomb models. This can be illustrated more easily for discrete straight lines and segments. Let a 2D discrete line $g^D$ in the 2D discrete hexagonal space be given. To each 2-hexel corresponds a rhombus with the same center and with sides determined by the basis vectors of the space $Ob_1b_2$ (see Figure 15). This correspondence defines an (imaginary) rhomboidal discrete space $\overline{Ob_1b_2}$ with the same center and basis vectors, as shown in Figure 15. In it, the rhombuses with centers corresponding to the hexels of the given discrete line $g^D$ constitute a discrete line $\bar{g}$. If the normal vector $\mathbf{n}$ to the continuous line $g$ belongs to the cone $C_1$, then $\bar{g}$ is a standard discrete line

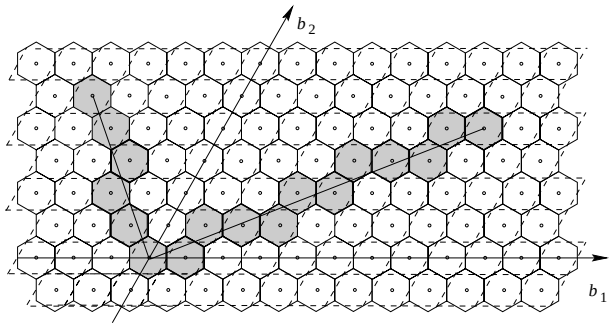


Fig. 15. Hexagonal discrete space with two discrete line segments in it, together with the corresponding rhomboidal discrete space.

in $\overline{Ob_1b_2}$. Otherwise, if $\mathbf{n} \in C_2$, $\bar{g}$ is a naive line in $\overline{Ob_1b_2}$. These kinds of lines can be generated through the well-known efficient linear algorithms for generation of standard and naive lines, respectively (see [6]). Because of the above mentioned one-to-one correspondence between 2-hexels and rhombuses, we obtain the centers of the hexels of the honeycomb discrete line. Thus the time-complexity of honeycomb discrete line generation matches the time-complexity of the algorithms for standard or naive line generation, depending on the cone to which the normal vector $\mathbf{n}$ belongs. Note that if $\mathbf{n} \in C_2$, we need to construct a naive discrete line in the rhomboidal model. Thus in this case the algorithm efficiency will be superior to the one for generation of 0-tunnel-free (standard) line within the classical square model. The above considerations easily extend to the two 3D honeycomb models of Section 4.1 and 4.2. Since in both models the hexels' centers form lattices, to each 3-hexel $h$ corresponds a parallelepiped which has the same center as $h$ and whose upper and lower faces are portions of the planes containing the two hexagonal faces of $h$. Thus we obtain a discrete 3D space $\overline{Oe_1e_2e_3}$ with the same center and basis as $Oe_1e_2e_3$, whose cells are parallelepipeds. With respect to this new (imaginary) space, one can search a plane discretization applying the well-known algorithms for generation of standard or naive planes, depending on the cone to which the projection of the normal vector to the plane belongs.

## 6 Concluding Remarks

We have proposed honeycomb models for raster graphics based on a hexagonal grid (resp. hexagonal prism tilings). We have shown how one can develop analytical discrete geometry within these models. In particular, we have defined lines (in the 2D space) and planes (in the 3D space). We have observed that the honeycomb models ensure discretizations, which are superior to the classical ones.

One can develop methods for discretizing more sophisticated objects (especially in $\mathbb{R}^3$), like 3D line segments, polygons and meshes of polygons. For this, one can appropriately modify certain discretization schemes and algo-

rithms, which have been developed for classical square/cubic models (see, e.g., [9,2,3,4]). Note that some problems that required long and complicated solutions within the classical model (see, e.g., [2,3]), in the new models can be handled more easily. The reason is that in honeycomb environment obtaining tunnel-free objects is easier, due to the properties of the honeycomb grids. In our opinion, the honeycomb models can serve as a useful alternative to the classical square and cubic models for a broad class of problems.

## References

[1] Andres, E., "Cercles Discrets et Rotations Discrètes," Thèse de Doctorat, Centre de Recherche en Informatique, Université Louis Pasteur, Strasbourg, France, 1992.

[2] Barneva, R.P., V.E. Brimkov, and Ph. Nehlig, "Thin Discrete Triangular Meshes," Theoretical Computer Science (Elsevier) **246** (1-2) (2000) 73–105.

[3] Brimkov, V.E., R.P. Barneva, and Ph. Nehlig, "Minimally Thin Discrete Triangulations," In: *Volume Graphics*, M. Chen, A. Kaufman, R. Yagel (Eds.), Springer Verlag (2000) Chapter 3, 51–70.

[4] Brimkov, V.E., and R.P. Barneva, "Graceful Planes and Lines," Theoretical Computer Science (Elsevier), to appear.

[5] Cohen, D., and A. Kaufman, "3D Line Voxelization and Connectivity Control," In: Proc. CG&A (1997) 1–24.

[6] Reveillès, J.-P., "Géométrie Discrète, Calcul en Nombres Entiers et Algorithmique," Thèse d'État, Université Louis Pasteur, Strasbourg, France, 1991.

[7] Saha, P., and A. Rosenfeld, "Strongly Normal Sets of Convex Polygons or Polyhedra," Pattern Recognition Letters, **19** (1998) 1119–1124.

[8] Sonka, M., V. Hlavac, and R. Boyle, "Image Processing, Analysis, and Machine Vision" (2nd Edition), IT Pu. Co., 1998.

[9] Stojmenovic, I., and R. Tosic, "Digitization Schemes and the Recognition of Digital Straight Lines," Hyperplanes and Flats in Arbitrary Dimensions. Digital Geometry. Contemporary Math. Series, Amer. Math. Soc. Providence, RI **1**19 (1991) 197–212.